Observation of residual disorder in the centre of amorphous solid water films after pore collapse at 125K

S. Townrow and P.G. Coleman*

Department of Physics, University of Bath, Bath BA2 7AY, UK

***email: p.g.coleman@bath.ac.uk**

Abstract

The rapid structural re-organisation of porous amorphous solid water, grown to thicknesses in the range 2.5-70 μm by vapour deposition on a copper substrate at 75K, after heating to 125K has been found to leave a μm-wide band of residual disorder – for example, nm-sized closed pores - in the centre of the film. This layer was revealed by thinning the film by sublimation and continuously measuring the fraction of 1.5 keV positrons implanted into the film which forms ortho-positronium in the top 150nm and decay into three gamma photons.

1. Introduction

The intriguing structural characteristics of water ice, and the transformations between different morphologies at temperatures above 120K continue to be the subject of research using many different spectroscopies, the majority being focussed on nm-scale films deposited on atomically flat surfaces [1,2]. While there is a degree of consensus, there remains significant discussion on basic features such as the glass transition [3], crystallisation kinetics [4,5] and the nature of the crystalline state below 180K [6,7]. It therefore seemed apposite to direct the technique of positronium (Ps) annihilation spectroscopy - whose efficacy in probing the sub-nanoscale structure and porous features of amorphous and crystalline water ice films has been established [8-10] - towards these long-standing issues, in an attempt to shed new light on them. In doing so a new and unexpected feature has been observed after re-organisation associated with pore collapse in amorphous solid water (ASW).

2. Experimental method

The principle of the spectroscopy is the measurement of the fraction F of mono-energetic positrons of energy E implanted normally into the sample which forms the spin triplet state of Ps, ortho-Ps, and subsequently decays into three gamma photons [11]. In the absence of nm-sized closed or interconnected pores, this can only happen by ortho-Ps diffusing through the ice and decaying in the vacuum above. Any lattice defects which trap the positrons and prevent them from forming ortho-Ps, or which trap the Ps and prevent its diffusion to the surface, reduce F - which is therefore a sensitive measure of disorder, for example in ice films grown at different rates or temperatures [11]. A degree of depth sensitivity is provided by changing E in the range 1.5 – 30 keV, corresponding to mean probed depths from ~ 75 nm to 10 μm.

The ice films were grown typically at a rate of ~7 nm s^{-1} to thicknesses in the range 2.5 - 70 μm by freezing distilled, de-ionised water vapour on to a machine-polished, and thus atomically rough, copper substrate held at 75K. Film thickness measurement is detailed in Ref. [10]. At this growth temperature the ice is highly porous; some pores are closed, with characteristic dimensions in the few to several nm range, while others are interconnected, sometimes providing channels leading to the surface [2]. The as-grown films were all then held at 125K for 10 mins, which leads to the collapse of the pore structure [12]. In common terminology, this would be porous ASW becoming 'sintered ASW' or a collapsed state similar to Hyperquenched Glassy Water (HGW), both being forms of Low-Density Amorphous (LDA) ice. This pore collapse is seen, in line with our earlier published work [13], as a sudden significant fall in *F* at 125K at all *E* (e.g., from ~20 to 3% at 2keV). In highly porous ASW ortho-Ps decay into three gamma photons can occur via migration through interconnected pores to the surface, or in large (~10nm diameter) closed pores in the bulk; both these channels are closed after pore collapse, and Ps has then to diffuse through the sintered ASW to reach the surface, with a probability much reduced by Ps trapping in open-volume atomic-scale defects and by positron trapping prior to Ps formation.

3. **Results and discussion**

An unexpected observation, illustrated in Fig.1, was made when 20μm films were grown at 75K, held at 125K for 10 mins, and then raised to temperatures between 166 and 184K. Here *E* = 1.5keV, corresponding to a mean positron implantation depth of ~75nm, so that ortho-Ps is being formed in the top 150nm or so of the film. At the temperatures chosen the films will have passed through the amorphous-to-crystalline transition, and they also sublime as the measurements proceed. The positrons are thus probing, continuously, 150 nm-wide slices of the films as they are revealed by sublimation, from the surface to the substrate.

The times taken for the films to sublime are very different at the different temperatures chosen, but because *F* falls to ~ 0 when the entire film has sublimed one can plot the data for different temperatures on a normalised scale representing the fraction of the film sublimed on a scale of 0 to 1. The unexpected feature in these data is the sharp and significant dip in *F* corresponding to a severely disordered layer in the centre of the films extending across approximately 7% of the film thickness. Evolution of the shape of the central layer with time at temperature – essentially a fractional narrowing - can be seen in the data for thicker films in the right-hand inset of Fig.1, eventually exhibiting the structure seen for the 67 μm film enlarged in the left-hand inset in the figure.

The higher values of *F* in the top half of the films indicates that defects there are readily annealed away on heating to above 155 K, and the asymptotic value of around 0.35 reflects optimum ortho-Ps diffusion through crystalline ice. Within ~ 5 μm of the centre of the films *F* falls rapidly, reflecting surviving disorder in this region, in a way which is similar in all the films shown. The lower values of *F* in the half of the films closer to the substrate interface are attributed to a higher density of surviving defects; the general increase seen as the film-substrate interface is approached – i.e., with time at temperature – reflects the progressive annealing of trapping sites. The different levels of *F* in the lower halves of the 20 μm films are again associated with defect annealing at the seven different measurement temperatures,. Defects in the lower half of the films do not anneal away as readily as those in the top half, even after several days at 172K, indicating that the defect structures in the two halves are different. It appears that if the defects cannot be annealed out prior to crystallisation, on heating to 172 K, they become effectively locked in place. Defect annealing is slowest in the thin central layer, indicating the higher concentration and/or size of the defects there.

To determine whether the dip is truly positioned in the centre of the films, irrespective of thickness or measurement conditions, or simply related to a time-dependent phenomenon

which coincidentally places the response at half the film depth, a set of measurements was taken for a 7.5 μm film measured at 175 K (see Fig.2). For each experimental run the ambient pressure was changed so that the time taken to complete each measurement (being proportional to the sublimation rate) was controlled in the range ~4 to 16 hours. When the data were plotted against the fraction of the film remaining, as in Fig.1, the dip feature was found to be identically positioned in the centre of the films. Thus we can conclude that the defected layer is indeed centrally located and that the response in F is not a time-dependent phenomenon. Measurements of F at different positron energies E support this model; response to the dip appears at earlier times for higher E; higher-energy positrons penetrate more deeply and therefore reach the defected layer before those with lower E. If the dip were time-dependent then the response would be similar at all E.

We now turn to the questions of when in the growth/measurement process the central defected layer is formed.

To answer this question a set of twin film samples were grown. Noting that the dip feature in F is only seen in films which have been grown at 75K and annealed at 120 or 125K for 10 minutes (compare with the featureless data for films grown at temperatures above 125K in Ref. [10]) a 10 μm film was grown at 75K, raised to 125K for 10mins and then held at the intermediate temperature T_{int} between 145 and 175K for a further 10 mins. The sample was then cooled again to 75K and a second 10 μm film grown on top of the first, the twin film then being held at 125K for another 10 mins and then raised to/sublimed at 172K for the measurements shown in Fig.3.

Fig.3 shows that without going through the T_{int} step there is a clear and significant dip 75% of the way through the twin film layer – i.e., in the centre of the first film grown (the 'lower film'). F values on the two sides of this dip lie on the same line, again slowly increasing with

time as trapping sites are annealed. This implies that the characteristics of the lower film have almost been 'frozen' – and that *F* here reflects the quality of the film immediately after annealing at 125K for 10 mins. A second dip is seen at the film-film interface, i.e. at the middle of the twin film structure, but then in the top film *F* exhibits an increase similar in shape to those seen for the top halves of single films in Fig. 3; no dip is seen in the middle of this film.

For T_{int} = 145K the *F* data are very similar to those for 125K. In contrast, for T_{int} =175K 10 mins is long enough for *F* to increase markedly in the top half of the lower film and a dip appears near the centre of the top film. The latter is thus behaving as a separate film (i.e., independently of the lower film) – presumably as a result of the change in the nature of the film-film interface.

For T_{int} = 155K the data (not shown, for clarity) show a sizeable but incomplete increase between 0.65 and 0.75 of the twin film structure. This implies that the change in structure which results in the increase in *F* above the first dip occurs rapidly when the region concerned has a free vacuum surface and at temperatures above ~ 155K, and that the change propagates from the central dip and not from the free surface.

One can therefore conclude that the central dips in *F* are formed rapidly on heating the porous ASW structure to 125K for 10 mins. At depths beneath the dips the only subsequent changes result from slow defect annealing (as illustrated in both Figs. 1 and 2). In the top halves of the films – those with a free film-vacuum interface - significant reorganisation is seen which allows defects to anneal prior to crystallisation and *F* to increase markedly, a change which appears to begin at the central defected layer, possibly because of the concentration of seeds for crystallisation associated with the disorder there. These changes in response above and below the central layer serve only to accentuate the characteristic shape of the dip in *F*.

We now consider the possible nature of the defects in the central layer. We know that these defects serve to impede strongly the formation of ortho-Ps or its migration to the vacuum. Whilst the former may proceed via positron trapping in atomic-scale open-volume defects it is not clear that this would necessarily suppress ortho-Ps formation. The strongest candidate is a layer of closed pores whose average size (probably ≤ 1 nm) is small enough to ensure that the majority of ortho-Ps existing in the pores are quenched (by pick-off interactions at the walls) into two-gamma decay. Any large or interconnected pores would serve to increase F, either allowing ortho-Ps to decay naturally within them or permitting migration along paths leading to the revealed surface during measurement.

Referring to Fig.1, one must conclude that the open-volume defects which congregate in the centre of the film following pore collapse at 125K do not migrate as effectively as those in the lower half of the film; indeed, some of the smaller defects in the lower half may be migrating to the centre where small pores ripen and grow. A similar agglomeration of vacancies into less mobile point defects in the centre of the damaged region has been seen in ion-implanted silicon [14].

It is possible to achieve a broad estimate of the concentration of closed pores of mean diameter D in the central region by invoking the diffusion-limited trapping model, which assumes that any Ps atom encountering a pore will be trapped with 100% probability [15]. The trapped Ps fraction $f = K/(K + \lambda)$, where K is the ortho-Ps trapping rate and λ its annihilation rate in un-defected ice. $K = 2\pi D\lambda L^2 N$, where D is the pore diameter, L is the ortho-Ps diffusion length in un-defected ice (185nm [11]), and N is the pore concentration. Combining these two expressions yields $N = f / [2\pi DL^2 (1\text{-}f)]$. Now F for good crystalline ice is ~30%, and at the dip falls to ~12%, so that $f \sim 3/5$. Thus $N \approx (7\text{x}10^{21})/D$ m^{-3}, with D in nm.

Finally we turn to the mechanism by which the central defected layer is formed. Our favored model first assumes that many small voids/vacancies are left after pore collapse, and that these are uniformly spread. This is supported by our observation that *F* for porous ice decreases suddenly on pore collapse, reflecting trapping by residual defects [13]. We now speculate that an amorphous-amorphous transition associated with pore collapse, perhaps ASW to HGW or some other form of LDA ice, progresses inwards from the two external surfaces – these regions having fewer bonds to break in order to reorganise. The transition wave promotes the migration of defects towards each other until they meet in the centre, where they agglomerate and become immobile. The data suggest that this reorganisation leaves a tail of defects above the central zone and defects with a higher average concentration or size below, possibly as a result of the very different nature of the two interfaces.

4. **Conclusions**

The authors hope that the unexpected observation of the central defected layer following ASW compaction at 125K will stimulate further study of ice films by Ps annihilation spectroscopy. Other models of defect migration and agglomeration in the centre of water ice films are certainly possible and it is to be hoped that these will be addressed by future theoretical investigations. Experimentally, it will be interesting to probe whether the central defect layer is a general phenomenon or restricted to pure LDA water ice films, and whether the substrate type and roughness play any significant role. The application of this technique to the study of ice films is in its infancy, but the intriguing nature of the results presented here suggest that there is tremendous scope for extending the spectroscopy and linking it with other in-situ techniques.

Acknowledgements

This research was supported by EPSRC, UK under grant no. EP/1016767/1. The authors would like to thank Prof. Martin Chaplin for helpful communications and for his valuable website *Water Structure and Science (http://www1.lsbu.ac.uk/water/)*.

[1] Scott Smith R, Matthiesen J, Knox J and Kay B D 2011 *J.Chem.Phys.*A **115** 5908-17

[2] Bartels-Rausch T *et al* 2012 *Rev.Mod.Phys.* **84** 885-944

[3] Sepúlveda A, Leon-Gutierrez E, Gonzalez-Silveira M, Rodríguez-Tinoco C, Clavaguera-Mora M T and Rodríguez-Viejo J 2012 *J.Chem.Phys.* **137** 244506

[4] Kondo T, Kato H S, Bonn M and Kawai M 2007 *J.Chem.Phys.* **126** 181103

[5] Moore E B and Molinero V 2010 *J. Chem. Phys.* **132** 244504

[6] Thürmer K and Nie S 2013 *Proc. Natl Acad. Sci. USA* **110** 11757-62

[7] Kuhs W F, Sippel C, Falenty A and Hansen T C2012 *Proc. Natl Acad. Sci. USA* **109** 21259-64

[8] Eldrup M, Vehanen A, Schultz P J and Lynn K G 1985 *Phys. Rev.* B **32** 7048-64

[9] Wu Y C, Jiang J, Wang S J, Kallis A and Coleman P G 2011 *Phys. Rev.* B **84** 064123

[10] Townrow S and Coleman P G 2014 *J. Phys.: Condens. Matter* **26** 125402

[11] Townrow S and Coleman P G 2013 *Rev. Sci. Instrum.* **84** 103908

[12] Mitterdorfer C, Bauer M, Youngs T G A, Bowron D T, Hill C R, Fraser H J, Finney J L and Loerting T 2014 *Phys. Chem. Chem. Phys.* **16** 16013

[13] Wu Y C, Kallis A, Jiang J and Coleman P G 2010 *Phys. Rev. Lett.* **105** 066103

[14] Krause-Rehberg R, Börner F and Redmann F 2000 *Appl. Phys. Lett.***77** 3932-34

[15] Coleman P G, Chilton N B and Baker J A 1990 *J. Phys.: Condens. Matter* **2** 9355-61

Figure captions

Figure 1. Ortho-Ps three-gamma fractions *F* measured as a function of time, converted to fractions of film thickness removed, for 20 μm films grown at 75K, held at 125K for 10 mins, and then raised to measurement temperatures between 166 and 184K. Left-hand inset: detail of the central dip for a 67 μm film. Right-hand inset: data for 5, 18 and 67 μm films.

Figure 2. Ortho-Ps three-gamma fractions *F* measured as a function of time, converted to fractions of film thickness removed, for 7.5 μm films grown at 75K, held at 125K for 10 mins, and then raised to the measurement temperatures of 175K. Zero = no suppression of sublimation (run time ~4h): low = low suppression of sublimation (run time ~ 6h): high = high suppression of sublimation (run time ~ 16h).

Figure 3. Ortho-Ps three-gamma fractions *F* measured as a function of time, converted to fractions of total film thickness removed, for twin 10 μm films (total thickness 20 μm). Both halves of the films were grown at 75K, raised to 125K for 10mins, but the lower halves were additionally held at intermediate temperatures between 145 and 175K for a further 10 mins. Measurement temperature = 172K.

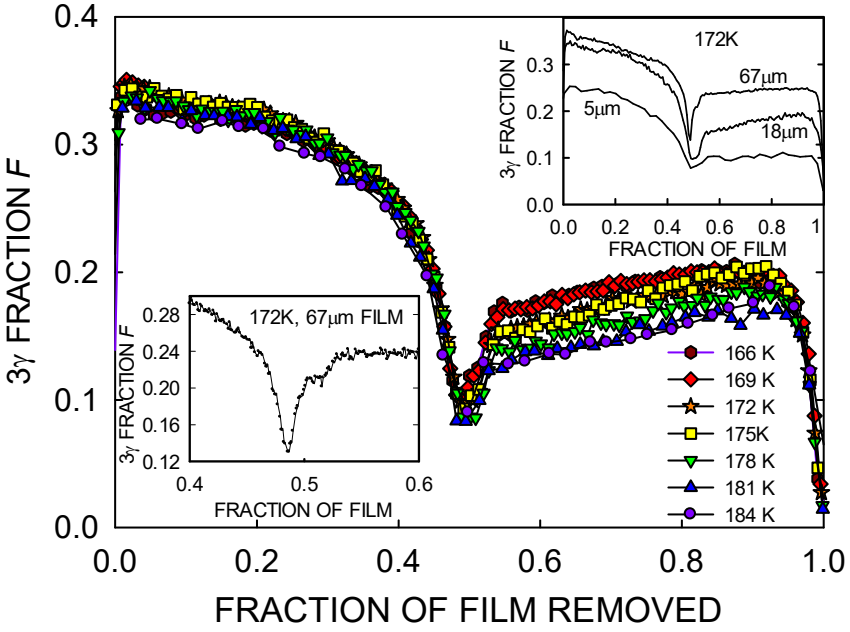
0.4
0.3
0.2
0.1
0.0
3γ FRACTION F
0.0
0.2
0.4
0.6
0.8
1.0
FRACTION OF FILM REMOVED
166 K
169 K
172 K
175K
178 K
181 K
184 K
172K
67μm
5μm
18μm
3γ FRACTION F
FRACTION OF FILM
172K, 67μm FILM
3γ FRACTION F
FRACTION OF FILM

Fig. 1

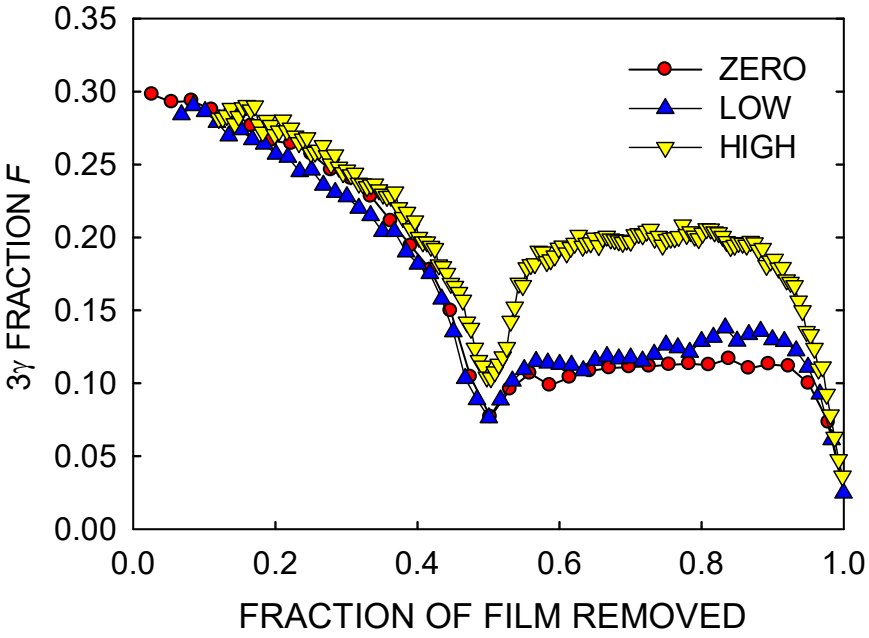
0.35
0.30
0.25
0.20
0.15
0.10
0.05
0.00
3γ FRACTION F
0.0
0.2
0.4
0.6
0.8
1.0
FRACTION OF FILM REMOVED
ZERO
LOW
HIGH

Fig. 2

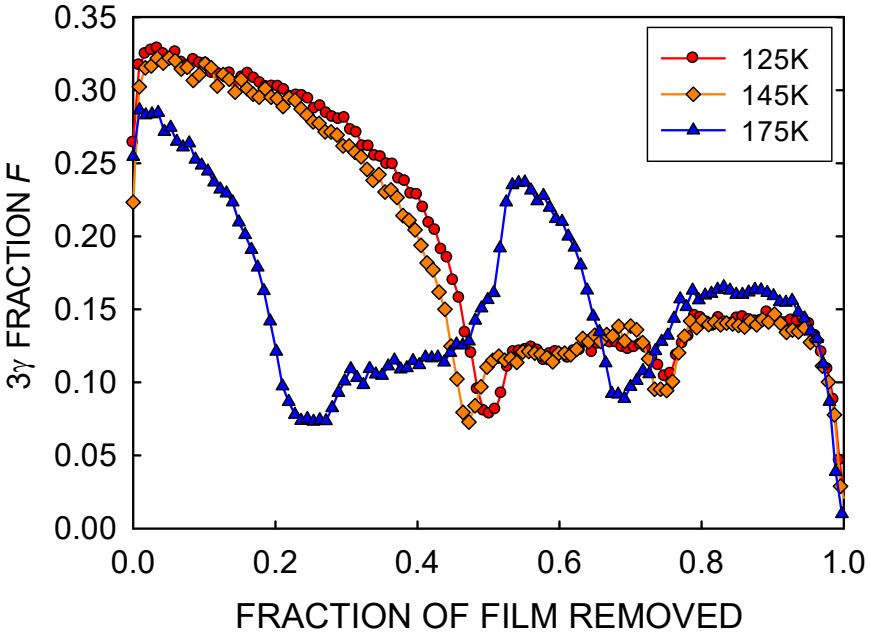
0.35
0.30
0.25
0.20
0.15
0.10
0.05
0.00
3γ FRACTION F
0.0
0.2
0.4
0.6
0.8
1.0
FRACTION OF FILM REMOVED
125K
145K
175K

Fig. 3